Documentation: A short explanation of the short code[†]

C. Weng[‡]

June 6, 2021

Abstract

The purpose of the code is to calculate (non-compact) finite difference weights using the method of undetermined coefficients for equispaced grids. The methodology is briefly described in this documentation. For more details the reader is referred to a text book such as Hirsch [1, chapter 4] or Chung [2, chapter 3].

1 Basic formula

Consider a function $u(x)$ and its n-th order derivative at point x. We want to estimate the derivative at x_0 with the explicit finite difference method (FDM). If the spatial discretization is performed with uniform grids (i.e. $x_i = x_0 + i\Delta x$, $i = \cdots -2, -1, 0, 1, 2\cdots$), then the general form of FDM may be written as

$$\left.\frac{\mathrm{d}^n u}{\mathrm{d}x^n}\right|_{x=x_0} \approx \frac{\cdots + a_{-2}u_{-2} + a_{-1}u_{-1} + a_0 u_0 + a_1 u_1 + a_2 u_2 + \cdots}{(\Delta x)^n} = \frac{1}{(\Delta x)^n}\sum_{i=\mathcal{L}}^{\mathcal{U}} a_i u_i, \tag{1}$$

where $u_i = u(x_i)$ is the value of u at x_i, $\mathcal{L}$ and $\mathcal{U}$ are respectively the lower and upper bounds of i, and

$$\frac{1}{(\Delta x)^n}[\cdots a_{-2}, a_{-1}, a_0, a_1, a_2 \cdots] \tag{2}$$

are the FDM weights to be determined.

The determination of the weights is closely related to the stencil we choose. The stencil tells which grid points in the neighborhood of x_0 are used to evaluate the finite difference Eq. (1). In general, the size of the stencil determines the accuracy of the FDM scheme for a given derivative order n. Take the central finite difference as an example, the stencil* $[-1, 0, 1]$ for $n = 1$ yields a 2nd order of accuracy, whereas the stencil $[-2, -1, 0, 1, 2]$ for the same n yields a 4th order of accuracy. One may increase the stencil size by including more neighboring points of x_0. If x_0 is "far" from the boundary of the computational domain, the expansion of the stencil can be performed at both sides of x_0. If x_0 is at or close to the boundary, however, one may need to employ a nonsymmetric stencil (such as $[0, 1, 2, 3, 4]$ and $[-1, 0, 1, 2, 3]$ for x_0 at and next to the left boundary respectively), and extend the size of the stencil in one direction to increase the FDM accuracy. Since FDM weights for nonsymmetric stencils are rarely tabulated in the literater, the current code is designed to calculate a_i for (hopefully) arbitrary stencils and derivative orders.

In the current code the calculation of a_i is based on Taylor-series expansions. For demonstration purposes, let us calculate the FDM weights for $n = 2$ and for the stencil $[-1, 0, 1, 2]$ by writing down the Taylor expansions of $u_{-1} = u(x_0 - \Delta x)$, $u_1 = u(x_0 + \Delta x)$, and $u_2 = u(x_0 + 2\Delta x)$ around x_0, and multiplying each with a_i:

$$a_{-1}u_{-1} = a_{-1}u_0 - a_{-1}u^{'}\Delta x + \frac{a_{-1}u^{''}}{2!}(\Delta x)^2 - \frac{a_{-1}u^{'''}}{3!}(\Delta x)^3 + \mathcal{O}\left[(\Delta x)^4\right], \tag{3a}$$

$$a_1 u_1 = a_1 u_0 + a_1 u^{'}\Delta x + \frac{a_1 u^{''}}{2!}(\Delta x)^2 + \frac{a_1 u^{'''}}{3!}(\Delta x)^3 + \mathcal{O}\left[(\Delta x)^4\right], \tag{3b}$$

$$a_2 u_2 = a_2 u_0 + a_2 u^{'} 2\Delta x + \frac{a_2 u^{''}}{2!}(2\Delta x)^2 + \frac{a_2 u^{'''}}{3!}(2\Delta x)^3 + \mathcal{O}\left[(\Delta x)^4\right]. \tag{3c}$$

Comparing Eq. (3) with Eq. (1), one may observe that the 2nd order derivative $u^{''} = \mathrm{d}^2u/\mathrm{d}x^2$ can be written in the form of Eq. (1) if the summation of Eq. (3a) to Eq. (3c) cancels out all other terms involving $u^{'}$, $u^{'''}$,

[†]First version: May 23, 2017.

[‡]German Aerospace Center (DLR), Institute of Propulsion Technology, Engine Acoustics, D-10623 Berlin, Germany.

*The stencil here is represented by the position index i.

$u^{''''}$...i.e. the red terms; the term $a_0 u_0$ in Eq. (1) would emerge if $a_{-1}+a_1+a_2=-a_0$. This yields the following equations for a_i

$$a_{-1}+a_0+a_1+a_2=0. \tag{4a}$$

$$-a_{-1}+a_1+2a_2=0,\ \text{(to cancel out } u^{'}\text{)}, \tag{4b}$$

$$a_{-1}+a_1+2^2a_2=2!,\ \text{(to remain } u^{''} \text{ with unit coefficient)}, \tag{4c}$$

$$-a_{-1}+a_1+2^3a_2=0,\ \text{(to cancel out } u^{'''}\text{)}, \tag{4d}$$

Because the size of the stencil is only four, we cannot exactly cancel more higher order derivative terms (otherwise we are left with an overdetermined system). These terms are therefore truncated in order to derive the FDM scheme Eq. (1), and the truncation error is indicated by the leading error term. In the above demo case, the leading error terms are those with $u^{''''}$, so the truncation error is $\mathcal{O}[(\Delta x)^2]$ and the FDM scheme is said to be 2nd order of accuracy. This is more clearly seen by writing down the FDM scheme with the coefficients calculated from Eq. (4), i.e.,

$$u^{''}=\left.\frac{\mathrm{d}^2u}{\mathrm{d}x^2}\right|_{x=x_0}=\frac{1}{(\Delta x)^2}\sum_{i=-1}^{2}a_iu_i+\mathcal{O}\left[(\Delta x)^2\right]\approx\frac{1}{(\Delta x)^2}\sum_{i=-1}^{2}a_iu_i. \tag{5}$$

Based on Eq. (4), we can further generalize the derivative of the FDM weights for a stencil $\boldsymbol{\sigma}=[\sigma_1,\sigma_2,\cdots\sigma_s]=[\mathcal{L},\cdots-1,0,1,\cdots\mathcal{U}]$ with size $s>n$, where $\mathcal{L}\leqslant 0$, $\mathcal{U}\geqslant 0$, and $\mathcal{U}-\mathcal{L}\geqslant 1$. That is, the the coefficients a_i in Eq. (1) are obtained by solving the following linear equation

$$\begin{bmatrix} 1 & 1 & \cdots & 1 & 1 \\ \sigma_1 & \sigma_2 & \cdots & \sigma_{s-1} & \sigma_s \\ \sigma_1^2 & \sigma_2^2 & \cdots & \sigma_{s-1}^2 & \sigma_s^2 \\ & & \vdots & & \\ \sigma_1^{s-1} & \sigma_2^{s-1} & \cdots & \sigma_{s-1}^{s-1} & \sigma_s^{s-1} \end{bmatrix}\begin{bmatrix} a_{\mathcal{L}} \\ a_{\mathcal{L}+1} \\ \vdots \\ a_{\mathcal{U}-1} \\ a_{\mathcal{U}} \end{bmatrix}=\begin{bmatrix} 0 \\ 1!\,\delta(1-n) \\ 2!\,\delta(2-n) \\ \vdots \\ (s-1)!\,\delta(s-1-n) \end{bmatrix}, \tag{6}$$

where δ is the Kronecker delta. Eq. (6) is the core formula in the code `getNonCompactFDMWeights.m`.

2 Order of accuracy

The order of accuracy of the FDM scheme is in general $s-n$, but there are exceptions. For example, when $n=2$ and the stencil is $[-1,0,1]$, Eq. (6) reads

$$\begin{bmatrix} 1 & 1 & 1 \\ -1 & 0 & 1 \\ 1 & 0 & 1 \end{bmatrix}\begin{bmatrix} a_{-1} \\ a_0 \\ a_1 \end{bmatrix}=\begin{bmatrix} 0 \\ 0 \\ 2 \end{bmatrix}, \tag{7}$$

which gives $a_{-1}=1$, $a_0=-2$, and $a_1=1$. If we continue the equations by including another $u^{'''}$ term, the extra equation is $-a_{-1}+a_1=0$, which is exactly the 2nd equation in Eq. (7). Therefore, the leading error term is not the $u^{'''}$ term but the $u^{''''}$ term, the order of accuracy is hence not 1 but 2.

In the code, the following condition, which is the extra equation to Eq. (6), is checked

$$\begin{bmatrix}\sigma_1^s\sigma_2^s\cdots\sigma_{s-1}^s\sigma_s^s\end{bmatrix}\begin{bmatrix} a_{\mathcal{L}} \\ a_{\mathcal{L}+1} \\ \vdots \\ a_{\mathcal{U}-1} \\ a_{\mathcal{U}} \end{bmatrix}=0? \tag{8}$$

If the condition is unsatisfied, then the order of accuracy is $s-n$; otherwise the order of accuracy is $s-n+1$.

The user can generate a finite difference matrix with a specified order of accuracy. Symmetric stencil is used at interior grid points whereas nonsymmetric stencils are used at points close to and at the boundaries; see `getNonCompactFDmatrix.m`.

3 Some examples

3.1 Modified wavenumber

If one plans to use the non-compact FDM for simulations of wave propagations, he may need to keep in mind that, a high-order FDM scheme does not necessarily guarantee accurate numerical solutions. This is demonstrated in this subsection. For more details the reader may refer to a text book such as Tam [3].

It is well-known that the characteristics of wave propagation are found through the dispersion relation, which is usually sought by inserting the ansatz of the wave, $\exp(-\mathrm{i}kx)$, into the differential equations. Here $k = 2\pi/\lambda$ is the wavenumber, and λ is the wavelength. In order to describe accurately the wave propagation, the dispersion relation should be matched in the numerical simulation, i.e., the derivative of the ansatz should be estimated accurately.

The exact solution of the 1st derivative of the ansatz of the wave form is

$$\frac{\mathrm{d}\exp(-\mathrm{i}kx)}{\mathrm{d}x} = -\mathrm{i}k\exp\left(-\mathrm{i}kx\right), \tag{9}$$

whereas the non-compact FDM, according to Eq. (1), would give

$$\begin{aligned}\frac{\mathrm{d}\exp(-\mathrm{i}kx)}{\mathrm{d}x} &\approx \frac{1}{\Delta x}\sum_{i=\mathcal{L}}^{\mathcal{U}} a_i \exp[-\mathrm{i}k\left(x+i\Delta x\right)] \\ &= \left[\frac{1}{\Delta x}\sum_{i=\mathcal{L}}^{\mathcal{U}} a_i \exp\left(-\mathrm{i}ki\Delta x\right)\right]\exp\left(-\mathrm{i}kx\right) \\ &= -\mathrm{i}\tilde{k}\exp(-\mathrm{i}kx),\end{aligned} \tag{10a}$$

where

$$\tilde{k} = \frac{\mathrm{i}}{\Delta x}\sum_{i=\mathcal{L}}^{\mathcal{U}} a_i \exp[-\mathrm{i}ki\Delta x] \tag{10b}$$

is defined as the modified wavenumber, which apparently deviates from the exact wavenumber k. We say that dispersion relation is preserved if the difference between $\tilde{k}\Delta x$ and $k\Delta x$ is small.

In Fig. 1 the modified wavenumbers computed with six symmetric stencils are shown. As can be seen, decreasing the number of grids per wavelength, i.e. $2\pi/(k\Delta x)$, results in larger differences between the exact and the modified wavenumbers. To better the accuracy, higher order FDM schemes should be used. However, the higher is the scheme accuracy, the larger is the stencil size.

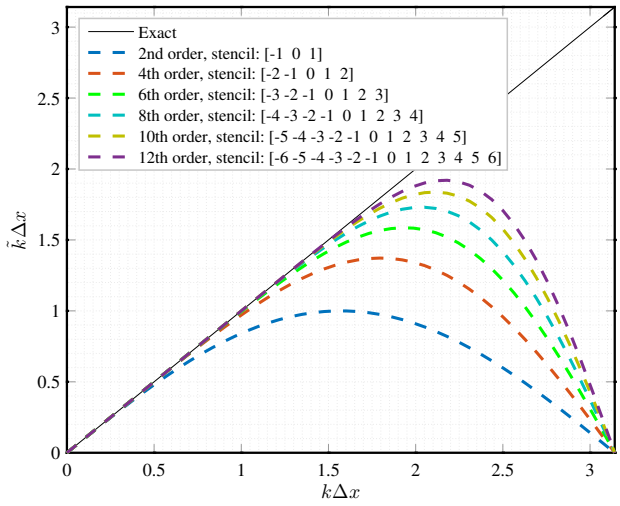

Figure 1. Modified wavenumbers computed with symmetric stencils.

There are some drawbacks of using stencils with large sizes. As may be indicated from Eq. (3), if one derives higher order schemes by using wider stencils, the coefficients of the higher order Δx polynomial terms increase. I.e, if central difference is used for $n = 1$, the leading error term in the Taylor expansion of $u_{\mathcal{U}}$ is $(s-1)^s\Delta x^s/(2^s s!)$, then the coefficient of the Δx^s term increases with s. This is one of the reason why in Fig. 1 the improvements of $\tilde{k}$ by increasing s "slow down" at larger s. Besides the inefficiency in increasing accuracies, wide stencils may face difficulties when being adapted to more complicated geometries. Is it possible to increase the order of accuracy while keeping the stencil "compact"? It seems to be possible. One may obtain high accuracy schemes with compact stencils with the Padé methods; see Lele [4]. Besides, one may also turn to the so-called Dispersion-Relation Preserving Schemes (DRP) which computes the finite difference schemes by minimizing the wavenumber error $E = \int_{-\pi/2}^{\pi/2} |\tilde{k}\Delta x - k\Delta x|^2 \mathrm{d}(k\Delta x)$; see Tam [3].

3.2 Convergence of the FDM on the problem of acoustic boundary layers

In spite of the disadvantages compared with other finite difference schemes, the non-compact FDM is still a widely used means of numerical simulations thanks to its handy features. For example, compared with the

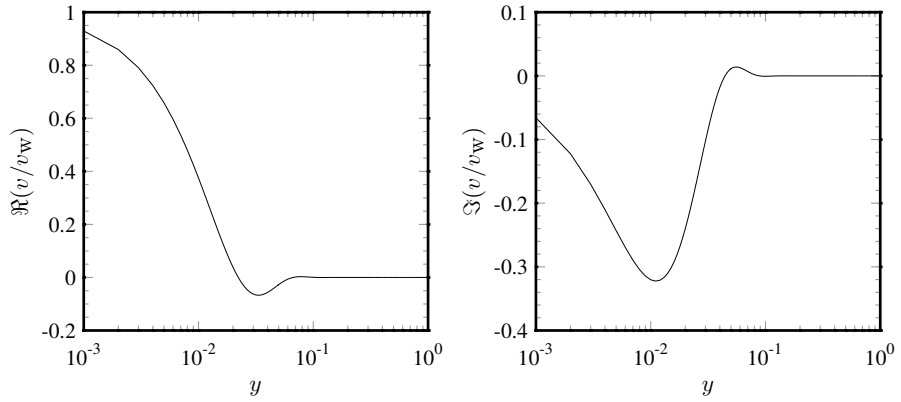

Figure 2. The asymptotic solution, as given in Eq. (12), to Eq. (11) for $\mathrm{Sh} = 100$.

compact FDM such as the Padé methods which are implicit schemes [i.e. the estimation of the derivative is not explicitly given as in Eq. (1)], the non-compact FDM can usually be applied to a given problem without including extra equations for the derivatives. Besides, the non-compact FDM enjoys some advantages over other popular numerical methods if the geometry of the given problem is not very complex. For example, compared with the finite element method the non-compact FDM can be implemented more straightforwardly without manipulating the governing equations of the problem; compared with the spectral method [5], the equation matrices obtained with the non-compact FDM are much sparser which considerably saves computer memory. Therefore, if the given problem has relatively simple geometries, the non-compact FDM is beyond any doubt a good choice for a hands-on of the problem.

Here an application of the non-compact FDM to a 1-D acoustic-boundary-layer is shown. The purpose is to examine the performance of the FDM near the boundary. Herein we assume that a wave is propagating in a channel with height $2H$; the boundary layer is so thin that the viscous shear wave vanishes at the channel center line. The governing equation and the boundary conditions of the viscous shear wave in the boundary layer is thus of the form (cf. Pierce [6, chapter 10])

$$\frac{\mathrm{d}^2 v}{\mathrm{d}y^2} - \mathrm{i}\,\mathrm{Sh}^2 v = 0, \tag{11a}$$

$$v = v_\mathrm{w} \text{ for } y = 0, v = 0 \text{ for } y = 1. \tag{11b}$$

where u is the velocity, y is dimensionless wall distance normalized by H, and Sh is the shear wavenumber [7]. Here we look at the asymptotic solution to Eq. (11) for large Sh which enjoys the simple form of

$$\frac{v}{v_\mathrm{w}} = \exp\left(-\sqrt{\mathrm{i}}\mathrm{Sh}\, y\right). \tag{12}$$

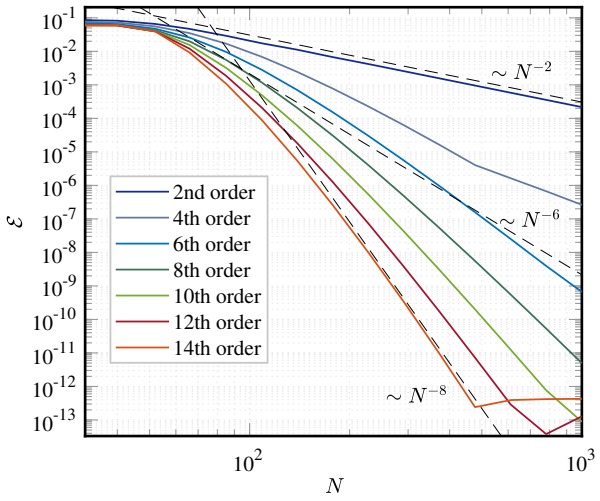

Figure 3. Numeric error $\mathcal{E}$ **for FDM schemes with different order of accuracies. The dashed lines are polynomials** $\sim N^{-2}, N^{-6}$ **and** N^{-8} **respectively.**

We compared the numerical solutions v_num to Eq. (11) with Eq. (12) for a "thin" boundary layer case by setting $\mathrm{Sh} = 100$, the asymptotic solution for which is shown in Fig. 2. The computational domain $y \in [0, 1]$ is discretized with N points, yielding a space vector $y_i = i\Delta y$ with $i = 0, 1, \cdots, N-1$. Various FDM schemes with different order of accuracies are used and compared. Let us define the max-norm error as

$$\mathcal{E} = \max_{0 \leqslant i < N} \left(\left| \frac{v(x_i) - v_\mathrm{num}(x_i)}{v_\mathrm{w}} \right| \right). \tag{13}$$

The maxima of the errors occur near the boundary $y = 0$ where the velocity v displays large gradients. The errors for the chosen FDM schemes are shown in Fig. 3. As expected, the FDM scheme with the higher order of accuracy converges faster with the increase of N, because the convergence rate is $\sim N^{-p}$ where p denotes the order of accuracy. Notice that for 12th and 14th order schemes their errors increase instead of decrease at larger N due to the reach of the machine epsilon.[†]

[†] https://en.wikipedia.org/w/index.php?title=Machine_epsilon&oldid=772013545 (accessed May 23, 2017).

References

[1] Charles Hirsch. *Numerical Computation of Internal and External Flows: The Fundamentals of Computational Fluid Dynamics*. Butterworth-Heinemann, Oxford, UK, 2nd edition, 2007. ISBN 9780750665940.

[2] T.J. Chung. *Computational Fluid Dynamics*. Cambridge University Press, New York, USA, 2nd edition, 2010. ISBN 9780521769693.

[3] C.K.W. Tam. *Computational Aeroacoustics: A Wave Number Approach*. Cambridge Aerospace Series. Cambridge University Press, 2012. ISBN 9780521806787.

[4] S. K. Lele. Compact finite difference schemes with spectral-like resolution. *Journal of Computational Physics*, 103(1):16 – 42, 1992. ISSN 0021-9991.

[5] C. Canuto, M. Y. Hussaini, A. Quarteroni, and T. A. Zang. *Spectral Methods: Fundamentals in Single Domains*. Springer-Verlag, Berlin Heidelberg, 2006. ISBN 978-3-540-30726-6. doi: 10.1007/978-3-540-30726-6.

[6] A. D. Pierce. *Acoustics: An Introduction to Its Physical Principles and Applications*. the Acoustical Society of America, New York, 1989. ISBN 0-88318-612-8.

[7] H. Tijdeman. On the propagation of sound waves in cylindrical tubes. *Journal of Sound and Vibration*, 39 (1):1–33, 1975. ISSN 0022-460X.